Eur. J. Biochem. 248, 872–878 (1997)


# Two-dimensional $^1$H-NMR and CD structural analysis in a micellar medium of a bovine $\alpha_{S1}$-casein fragment having benzodiazepine-like properties

Marc LECOUVEY[1], Céline FROCHOT[1], Laurent MICLO[2], Piotr ORLEWSKI[1], Alain DRIOU[2], Guy LINDEN[2], Jean-Luc GAILLARD[2], Michel MARRAUD[1], Manh Thong CUNG[1] and Régis VANDERESSE[1]

[1] Laboratoire de Chimie Physique Macromoléculaire, CNRS-URA 494, ENSIC-INPL, Nancy, France
[2] Laboratoire des Biosciences de l'Aliment, Unité associée à l'INRA, Université Henri Poincaré-Nancy 1, Vandœuvre lès Nancy, France

(Received 25 April/18 July 1997) – EJB 97 0595/3

The conformation of the benzodiazepine-like decapeptide, YLGYLEQLLR, corresponding to residues 91–100 of bovine $\alpha_{S1}$-casein, has been examined in SDS micelles using CD, two-dimensional $^1$H-NMR and restrained molecular-dynamics simulation. Evidence is presented that the decapeptide adopts a rigid structure in water/SDS micellar medium, but not in water or dimethylsulfoxide. The three-dimensional structure, consistent with the proton-proton distances obtained from the quantitative analysis of the two-dimensional NOEs, was generated by restrained energy minimization and molecular-dynamics simulation. In water/SDS micellar medium, YLGYLEQLLR adopts an amphipathic helicoid structure with distinct hydrophobic and hydrophilic faces. The relative disposition of the tyrosine aromatic rings was compared with that of the aromatic rings in the benzodiazepines.

*Keywords:* $\alpha_{S1}$-casein; benzodiazepine-like peptide; NMR; molecular dynamics; circular dichroism.

Being the primary food for young mammals, milk does not only afford a source of nitrogen for biosynthesis but also contains molecules with biological activities that play a key role in newborn development. These essential molecules are native proteins, involved in the absorption of nutriments or in anti-infectious mechanisms, and polypeptides, especially hormones, the roles of which are not totally elucidated in neonate development [1]. For most species, caseins are the main milk proteins and have been considered for a long time to be only nitrogen providers. However, since about 15 years ago, many authors have observed that enzymatic hydrolysis of caseins or whey proteins produces biologically active peptides such as opioid [2] and opioid-antagonist peptides [3], angiotensin-converting-enzyme inhibitors [4], immunostimulating peptides [5], platelet-aggregation inhibitors [6], casein phosphopeptides that are carriers of minerals ($Ca^{2+}$, $Fe^{2+}$) [7], and mitogenic [8] and antibacterial peptides [9]. These activities can be found in milk from several species. Some of these peptides have been shown to be produced *in vivo*. In rat, blood-pressure reduction has been demonstrated *in vivo* after fermented milk ingestion [10]. However, the physiological significance of such peptides in development of mammalian young remains to be determined.

Recently, it was observed that a tryptic hydrolysate of one of the major bovine casein, $\alpha_{S1}$-casein, decreases pentylenetetrazole-induced convulsions in Wistar rats, and displays a similar effect as diazepam in the plus-maze elevated test, a behavioral test revealing anxiolytic properties of drugs. Moreover, it has an affinity of about 100 μM for the benzodiazepine site of the type-A 4-aminobutyric acid (4Abu) receptor. Only residues 91–100 of $\alpha_{S1}$-casein (YLGYLEQLLR) carry that activity [11].

The type-A 4Abu receptor belongs to the family of ligand-gated ion channels. It mediates rapid chloride fluxes in response to 4Abu binding. In addition to the 4Abu site, the receptor has distinct binding sites for allosteric modulators, such as benzodiazepines, barbiturates and steroids. Via one of these allosteric sites, benzodiazepines potentiate type-A-4Abu-receptor mediated $Cl^-$ influx [12]. The pharmacological profile of benzodiazepine-receptor agonists consists of anxiolytic, anticonvulsivant, sedative and myorelaxant activities. For long-term use of benzodiazepines, tolerance to certain effects and physical dependence might develop. New agonists without these secondary effects should be of greatest pharmacological interest.

Because residues 91–100 of $\alpha_{S1}$-casein are probably critical for the benzodiazepine-like activity, the conformational properties of $\alpha_{S1}$-casein-(91–100)-peptide have been investigated by CD, $^1$H-NMR, and by energy minimization (EM) and restrained molecular dynamics (MD) using the NMR parameters (NOE and temperature-coefficient values) as geometrical constraints. Experiments in water or dimethylsulfoxide indicate that the peptide is essentially flexible. Addition of SDS in water results in a conformational transition toward a rather rigid, defined structure. This micellar medium is often presented as an elementary model mimicking the lipid-water interface of biological membranes [13]. The resulting MD average conformation is discussed with reference to that of the benzodiazepine derivatives [14, 15].

## EXPERIMENTAL PROCEDURES

**Peptide synthesis.** The YLGYLEQLLR decapeptide was synthesized on a Dupont Coupler 250 peptide synthesizer (Dupont Co.) from N$\alpha$-*tert*-butoxy-carbonyl(Boc)-mesitylene-2-sul-

*Correspondence to* R. Vanderesse, Laboratoire de Chimie Physique Macromoléculaire, CNRS-URA 494, ENSIC-INPL, BP 451, 1 rue Grandville, F-54001 Nancy Cedex, France
*Fax:* +33 3 83 37 99 77.
*E-mail:* r.vanderesse@lcpm.ensic.u-nancy.fr
*URL:* http:www.ensic.u-nancy.fr/ENSIC/LCPM/LCPM.html

*Abbreviations.* MD, molecular dynamics; 4Abu, 4-aminobutyric acid; Boc, *tert*-butoxycarbonyl; EM, energy minimization; Nitrazepam, 7-Nitro-1,3-dihydro-5-phenyl-2H-1,4-benzodiazepin-2-one.

fonyl-arginine-4-(hydroxymethyl)-phenylacetamidomethyl-polystyrene resin (0.56 mmol/g substitution, Neosystem), using Boc solid-phase peptide-synthesis protocols. The peptide chain was assembled starting from 0.5 mmol mesitylene-2-sulfonyl-arginine linked to the resin by 2 h coupling of the Boc-Xaa (1.5 mmol), with the side chains of Glu and Tyr protected by benzyl ester and 2,6-dichlorobenzyl ester, respectively, in the presence of 2-(1H-benzotriazole-1-yl)-1,1,3,3-tetramethyl-uronium tetrafluoroborate (1.5 mmol) and diisopropylethylamine (4.5 mmol) in dimethylformamide/dichloromethane (1:3). The completion of each coupling was monitored by Kaiser ninhydrin and 2,4,6-trinitrobenzenesulfonic acid tests. Deprotection of the Boc group was achieved by 40% (by vol.) trifluoroacetic acid in dichloromethane. A standard cleavage with 18% (by vol.) trimethylsilyl trifluoromethane sulfonate, 65% (by vol.) trifluoroacetic acid, 11% (by vol.) thioanisol and 6% (by vol.) 1,2-ethanedithiol afforded the crude peptide, which was desalted on Sephadex G-25 and eluted with the quaternary solvent *n*-butanol/pyridine/acetic acid/water (15:10:3:12). Reverse-phase HPLC was performed on a Merck L-6200 chromatograph coupled to a Jasco 875-UV detector, on a 1 cm×25 cm Merck Lichrocart column packed with Lichrospher WP300 RP-18 (5 μm) using a linear gradient from 69% to 39% acetonitrile in 0.1% (by vol.) trifluoracetic over 40 min (4 ml/min, 214 nm). Matrix-adsorption laser-desorption/ionization time-of-flight mass spectroscopy was carried out on a Bruker Protein TOF spectrometer: calculated, 1268.48 (M+1); found, 1268.27.

**Circular dichroism.** The peptide (79 μM) was investigated in sodium phosphate, pH 5.9, with increasing SDS concentrations up to 0.2 M. CD spectra were recorded at 25°C on a Jobin Yvon CD6 spectrophotometer using a 1-mm−path-length quartz cell, a 2-mm bandwidth, a scan speed of 4 nm/min, a time constant of 8 s, and four scan accumulations. The air baseline was recorded and subtracted after each series of four scans. All CD spectra are reported in terms of deg · $cm^2$ · $dmol^{-1}$.

**NMR spectroscopy.** The peptide (5 mM) was dissolved in three media: dimethylsulfoxide, sodium phosphate in $H_2O/D_2O$ (95:5), pH 6, and the same solution containing perdeuterated SDS. Tetramethylsilane and sodium trimethylsilyl-3-[2,2,3,4-$^3H_4$]-propionate were used as internal standards in dimethylsulfoxide and water, respectively. NMR experiments were performed at 25°C on a Bruker DRX-400 spectrometer, and data processing was achieved on a Silicon Graphics workstation using Bruker-UXNMR software. TOCSY and NOESY experiments were recorded in the phase-sensitive absorption mode with quadrature detection in both dimensions using the time-proportional phase-incrementation mode [16]. NOE build-up curves were constructed for four mixing times (100, 200, 350 and 500 ms) to determine the mixing-time interval where no spin diffusion occurs [17]. The water resonance was suppressed by the WATERGATE method (water suppression by gradient-tailored excitation) [18] incorporated in the TOCSY and NOESY sequences to keep the exchangeable proton signals. This WATERGATE sequence was composed of a field-gradient echo combining one selective 180° radio-frequency pulse and two short field-gradient pulses of the same amplitude (12 G/cm) and sign. The spectral width in $F_1$ and $F_2$ was 5000 Hz. 512 experiments with 2K data points in the $F_2$ dimension were performed, and data points $t_1$ were zero-filled to give a 1K×1K data matrix. On the basis of the NOESY cross-peak volumes, and assuming an isotropic motion with a single correlation time for all interacting spins, the interproton distances were calculated directly from the ratios of the corresponding cross-relaxation NOEs [17], and the interproton distance of 0.178 nm between the two Y94-C$\beta H_2$ geminal protons as a reference. The temperature coefficients for the NH proton resonances were measured in the water/SDS medium between 25°C and 68°C. Due to signal broadening, the geminal and vicinal proton coupling constants could not be determined.

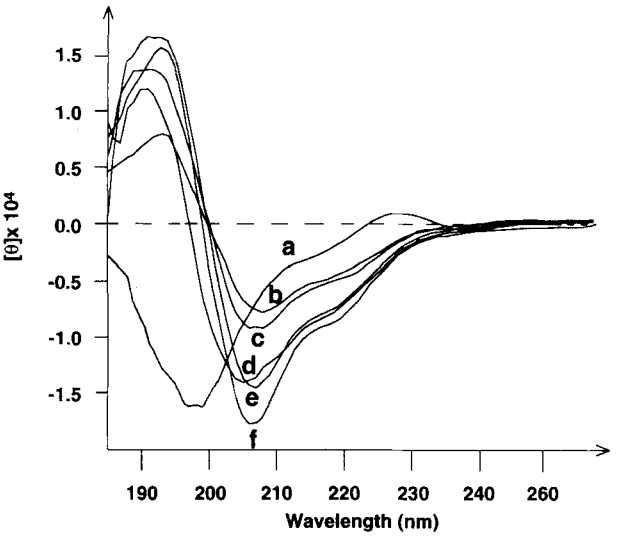


**Fig. 1. CD spectrum of the benzodiazepine-like decapeptide in water as a function of SDS concentration.** The peptide concentration was 79 μM. The SDS concentration was (a) 0.0, (b) 1.5, (c) 3 (d) 15, (e) 30 and (f) 200 mM.

**Molecular modeling.** The EM and MD calculations were performed on a Silicon Graphics workstation using Discover Biosym program. On the basis of CD analysis and NOESY results, the $3_{10}$ and $\alpha$ helices were built for $\alpha_{s1}$-casein-(91−100)-peptide. Both structures were submitted to 300 steps of steepest-descent restrained EM with a set of 39 backbone-backbone and 10 backbone-side chain distance constraints measured in a 200-ms NOESY experiment. Due to the probable flexibility of the side chains, the backbone-backbone and backbone-side chain constraints were associated with different force constants (5000 and 1670 kJ · $mol^{-1}$ · $nm^{-2}$, respectively). The backbone-backbone distance constraints from overlapping NOE cross-peaks were affected with a low force constant (1000 kJ · $mol^{-1}$ · $nm^{-2}$) and a large distance-constraint interval (0.08 nm) to avoid overestimation of their contribution in MD simulation. The two calculations converged toward quite similar conformers. The treatment was followed by a short series of *in vacuo* MD simulations of 0.1 ps each using the six-step temperature elevation (50, 100, 150, 200, 250 and 300 K). A 25-ps restrained MD under temperature control via the direct velocity scaling was performed. After thermal equilibration, a 320-ps restrained MD with weak coupling (0.1 ps) to the thermal bath was calculated. The 30-ps last period of MD simulation, which exhibited no substantial conformational changes, was used for conformational averaging and analysis. A $3r$ dielectric constant for coulombic interactions and a double cut-off at 1.25 nm and 1.4 nm for all non-bonded interactions were applied to the above calculations.

## RESULTS AND DISCUSSION

**Circular dichroism.** The dependence of the CD spectrum on SDS concentration in water is shown in Fig. 1. In pure water, the spectrum essentially presents a negative band at 198 nm, typical of an unordered conformation [19]. Upon a addition of SDS, even at concentrations below the critical micelle concentration (8 mM), a positive band at 192 nm and two negative bands, at 208 nm and 220 nm, appear. Their intensity increases progressively with SDS concentration, and reaches a plateau at

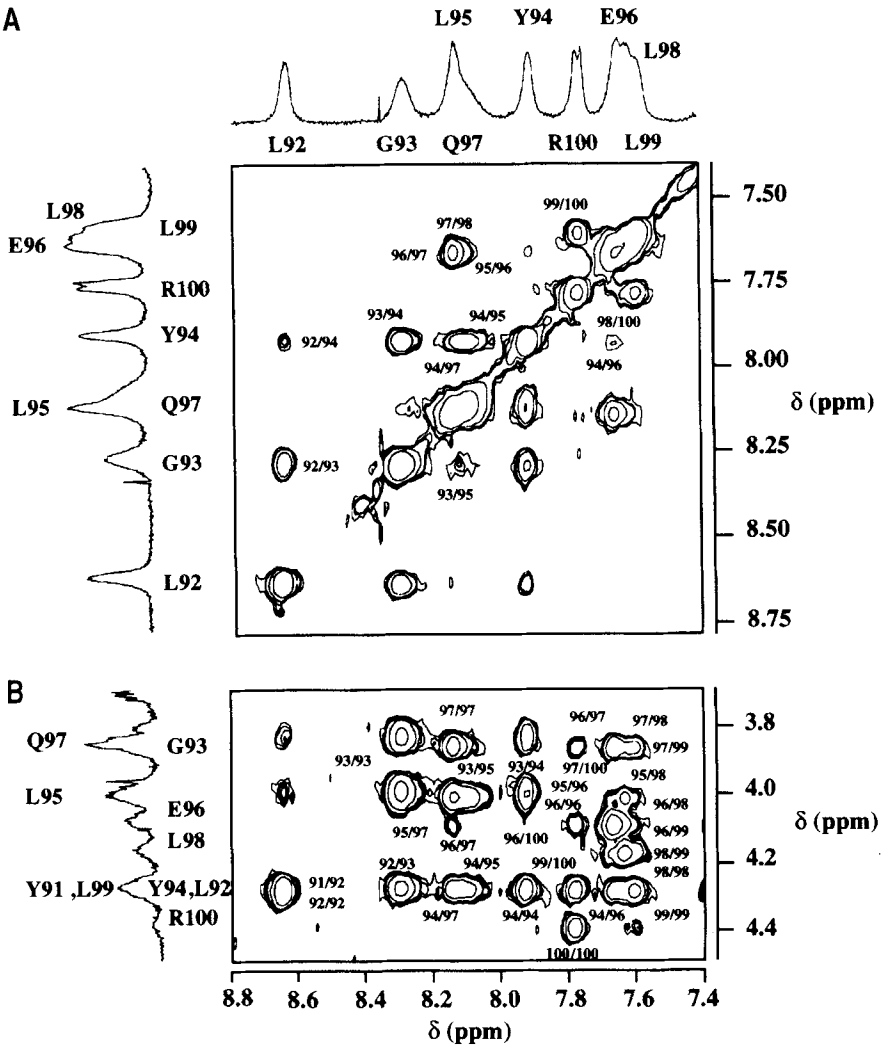


**Fig. 2. Portion of the decapeptide NOESY spectrum in SDS/water showing the NH/NH (A) and CαH/NH (B) NOE connectivities.** Peptide concentration, 5 mM; SDS concentration, 0.20 M; $\tau_m$ = 200 ms.

0.2 M SDS. This change indicates that the peptide experiences a conformational transition upon interaction with SDS micelles. In water/SDS, the positive band at 192 nm and the negative band at 208 nm have similar absolute magnitudes, and the latter is about twice as intense as the negative band at 220 nm. Such a spectrum profile is in favor of a $3_{10}$ helix rather than of an $\alpha$ helix [20]. However, the possibility of some $\alpha$ helix cannot be excluded completely since it is known that tyrosine may result in a weaker contribution at 220 nm [21].

**$^1$H-NMR.** The decapeptide in dimethylsulfoxide only exhibits a few NOE connectivities, indicating the absence of any preferred rigid structure in this strong solvating medium. In water, only few weak rotating-frame-Overhauser-enhancement connectivities are observed for long mixing times, and the absence of NH-NH correlations denote a flexible structure, in good agreement with the CD spectrum. The NOE connectivities that appear on addition of SDS in water reflect the peptide-micelle interaction and the restricted flexibility of the peptide in this medium.

The spin systems in water containing SDS (0.25 M) were delineated by COSY and TOCSY ($\tau_{cm}$ = 75 ms) experiments. The Y91/Y94 and L92/L95/L98/L99 spin systems were sequentially assigned from the $\alpha N(i,i+1)$ and $NN(i,i+1)$ backbone NOE connectivities (Fig. 2) [22]. The proton resonances are listed in Table 1, together with the NH temperature coefficients.

The temperature dependence $\Delta\delta/\Delta T$ for the NH resonances is often used to discriminate solvent-exposed (high absolute $\Delta\delta/\Delta T$ value) and solvent-shielded amide protons (small absolute $\Delta\delta/\Delta T$ value), which generally denote hydrogen-bonded NHs. The temperature coefficients listed in Table 1 reveal that the five C-terminal NHs are less solvent accessible than the four N-terminal NHs, in agreement with the hypothesis of a helicoid structure suggested by the CD experiments. The E96 and L98 NHs are expected to be involved in strong intramolecular interactions. The same holds true for the R100 NεH ($\Delta\delta/\Delta T = -1.8\times10^{-3}$ ppm/K) and one R100 Nη H guanidinium proton ($\Delta\delta/\Delta T = -1.6\times10^{-3}$ ppm/K), whereas the other three R100 guanidinium protons are in rapid exchange with water and not visible at room temperature. Therefore, the R100 NεH and one of the R100 Nη H protons are involved in strong intramolecular interactions, which could be a salt bridge with E96 $C\delta O2^-$ and/or R100 $CO_2^-$ [23]. The Q97 $N\varepsilon H_2$ carboxamide protons are moderately solvent exposed ($\Delta\delta/\Delta T = -4.1\times10^{-3}$ ppm/K and $-4.2\times10^{-3}$ ppm/K).

The particular pattern of short-range NOEs (Fig. 3) provides information on the secondary structure. As a general rule, helices are characterized by strong $NN(i,i+1)$ NOE cross-peaks, corresponding to short $NH_i$-$NH_{i+1}$ distances, and by medium or weak $\alpha N(i,i+1)$, $\alpha N(i,i+3)$ and $\alpha\beta(i,i+3)$ NOEs [24]. The $3_{10}$ helix differs from the $\alpha$ helix in the presence of medium

**Table 1. Proton NMR resonance assignments for $\alpha_{s1}$-casein-(91–100)-peptide (0.005 M) in $H_2O/D_2O$ (95:5) containing perdeuterated SDS (0.2 M, pH 6).** NH shifts ($\delta$) were measured from sodium trimethylsilyl-3-[2,2,3,3-$^2H_4$]propionic acid at 298 K. NH-shift temperature-dependance coefficients ($\Delta\delta/\Delta T$) are also listed.

| Residue | NH shift | $\Delta\delta/\Delta T$ | Chemical shift of | | | | | |
|---|---|---|---|---|---|---|---|---|
| | | | C$\alpha$H | C$\beta$H | C$\gamma$H | C$\delta$H | C$\varepsilon$H | Other NHs |
| | ppm | $10^{-3}\times$ppm/K | ppm | | | | | |
| Y91 | | | 4.27 | 3.30, 3.06 | | 6.87 | 7.20 | |
| L92 | 8.64 | −5.1 | 4.27 | 1.61 | 1.92 | 0.96 | | |
| G93 | 8.30 | −6.4 | 3.99, 3.84 | | | | | |
| Y94 | 7.92 | −4.4 | 4.27 | 3.09, 2.99 | | 6.80 | 7.07 | |
| L95 | 8.11 | −5.8 | 3.96 | 1.58 | 1.79 | 0.99, 0.92 | | |
| E96 | 7.66 | −1.4 | 4.05 | 2.08 | 2.36, 2.50 | | | |
| Q97 | 8.14 | −4.0 | 3.82 | 2.15 | 2.39, 2.54 | | | 6.82[a], 7.39[b] |
| L98 | 7.63 | −2.1 | 4.18 | 1.60 | 1.77 | 0.87 | | |
| L99 | 7.61 | −2.9 | 4.29 | 1.92 | 1.62 | 0.89 | | |
| R100 | 7.78 | −3.3 | 4.24 | 1.97, 1.87 | 1.62 | 3.21 | | 7.11[c], 6.48[d] |

[a] $\Delta\delta/\Delta T = -4.2 \cdot 10^{-3}$ ppm/K.
[b] $\Delta\delta/\Delta T = -4.1 \cdot 10^{-3}$ ppm/K.
[c] N$\varepsilon$H, $\Delta\delta/\Delta T = -1.8 \cdot 10^{-3}$ ppm/K.
[d] N$\eta$H, $\Delta\delta/\Delta T = -1.6 \cdot 10^{-3}$ ppm/K. Only one of the four R100 (N$\eta$H$_2$)$_2$ is visible at room temperature.

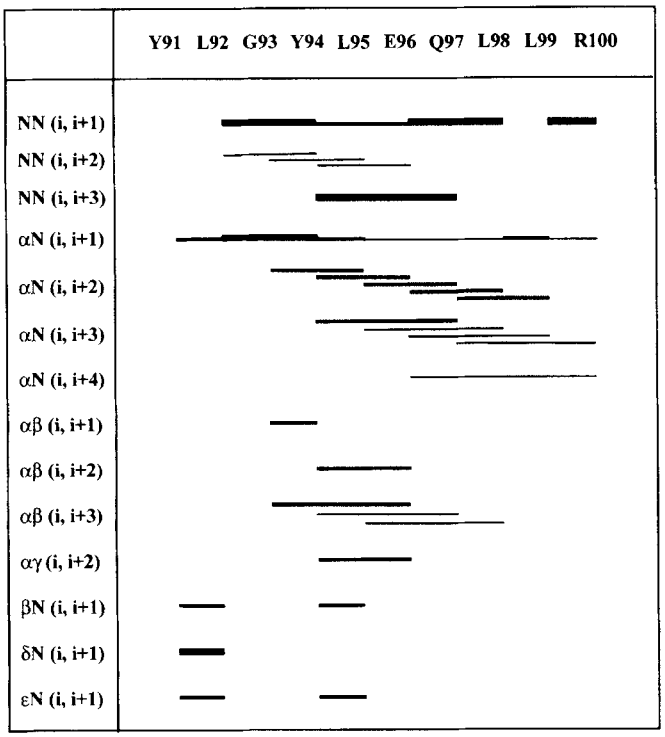


**Fig. 3. Summary of the $^1H/^1H$ NOE connectivities for the decapeptide in SDS/water.** The intensity of the NOE cross-peaks is indicated by the thickness of the lines, classified as strong, medium and weak.

$\alpha N(i,i+2)$ NOE connectivities for the former and weak $\alpha N(i,i+4)$ NOE connectivities for the latter. In addition, random sequences are characterized by the presence of strong $\alpha N(i,i+1)$ NOEs and the absence of other short-range NOEs involving the NH and C$\alpha$H protons [25].

In the present case, strong to medium $NN(i,i+1)$ and medium to weak $\alpha N(i,i+1)$ sequential NOE cross-peaks are observed with various medium and weak $NN(i,i+2)$, $NN(i,i+3)$, $\alpha N(i,i+2)$ and $\alpha N(i,i+3)$ NOE cross-peaks (Fig. 3). However, the partially superimposed resonances of the Y91, L92, Y94 and L99 C$\alpha$Hs, of the G93, L95 and Q97 C$\alpha$Hs, of the L95 and Q97 NHs, and of the E96, L98 and L99 NHs, prevent various eventual medium-range and long-range NOE connectivities being assigned because of their weak intensity, or of their superposition on other strong NOEs, or their close proximity to the diagonal, as for the L98-NH/L99-NH NOE cross peak. Except the weak G93-C$\alpha$H/E96-C$\beta$H NOE cross-peak, and due to the overlapping of the $\alpha$ and $\beta$ proton resonances for the residues of the same type (Y91/Y94, L92/L95/L98/L99 and E96/Q97), the other $\alpha\beta(i,i+3)$, NOEs are very weak or could not be identified. Nevertheless, the presence of successive medium $\alpha N(i,i+2)$ cross peaks argues for the occurrence of a $3_{10}$ helix from G93 to L99, which is confirmed by the small temperature coefficients for the last five C-terminal residues, compared with those for the N-terminal part of the molecule. The weak $\alpha N(i,i+4)$ E96-C$\alpha$H/R100-NH NOE cross-peak (Fig. 3) suggests that the C-terminal R100 residue could rather participate in an $\alpha$-helix fragment.

In agreement with the CD data, the NMR data indicate that most of the molecules probably adopt a helicoid conformation in the SDS/water micellar medium. Many examples of SDS-induced transitions from random to helical structures have been reported, although the SDS micelles do not seem to be capable of imposing an $\alpha$-helix structure on any sequence independent of its intrinsic folding tendencies [26, 27].

**Molecular modeling.** As a first approximation, the decapeptide molecule was constructed in canonical $3_{10}$-helix and $\alpha$-helix forms, from G93 to R100, which were used for starting restrained MD calculations based on 39 backbone-backbone and 10 backbone-side chain constraints with proton-proton estimated distances. In the absence of stereoassignment of the $\alpha$ and $\beta$ methylene protons, pseudoatoms with adjusted distance constraints were introduced. The first restrained energy-minimization steps of the $\alpha$ and $3_{10}$ helix led to two quite similar conformers, which were used subsequently as the starting structures for MD calculations.

Distance-restrained MD simulation of the decapeptide in SDS micellar solution was carried out for 320 ps to derive conformations consistent with the NMR data (interproton distances and NH proton accessibility). During the last 30-ps MD analyses the structural variations were only fluctuations about an average

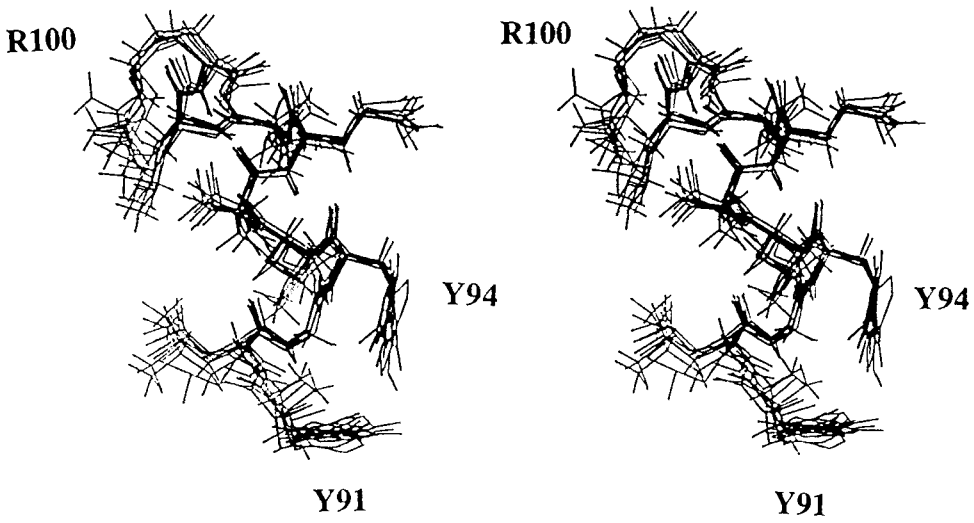


**Fig. 4. Ten superimposed structures of the decapeptide, extracted from the last 30 ps of restrained-MD simulation.**

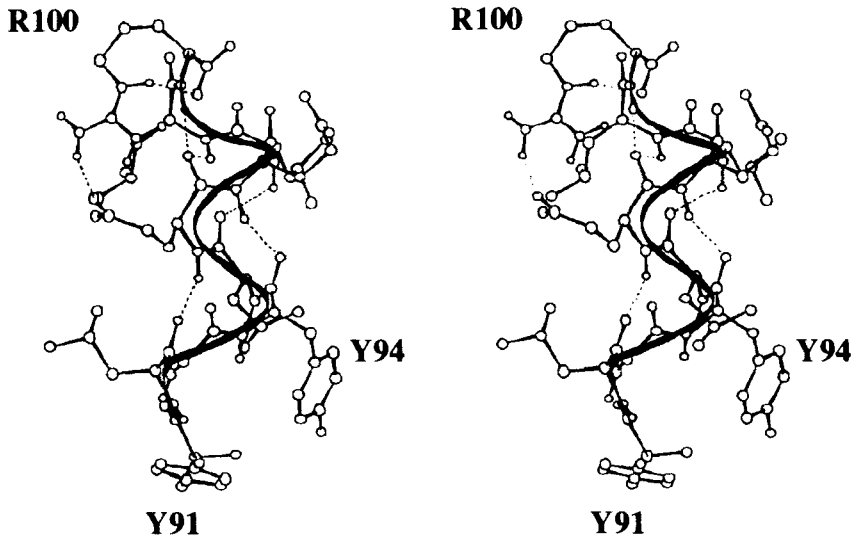


**Fig. 5. Stereoviews of the decapeptide time-averaged structure from the last 30 ps of restrained-MD simulation.**

conformation, as shown by the ten superposed conformers for every 3 ps of the 30-ps MD analysis (Fig. 4). As expected from the non-stereoassignment of the $\alpha$ and $\beta$ methylene protons, and from the lower force constant for the backbone-side chain constraints, the side chains were more agitated than the backbone. Similarly, due to the small number of distance constraints concerning the Y91 backbone, the N-terminal residue was relatively agitated.

This 30-ps MD analysis was used for further analysis and conformational averaging. The time-averaged structure was obtained from 150 conformers and subsequent energy minimization (Fig. 5). The residue-by-residue rmsd between the final average conformation and the 150 individual conformers was less than 0.03 nm when applied to heavy atoms. The interproton distances of the time-averaged structure are in good agreement with those deduced from the NOEs. Only six of them (two backbone-backbone and four backbone-side chain distances) are out of the margins by 0.029–0.045 nm, and the largest violations are observed for the backbone-side chain distances. Such differences are commonly observed for oligopeptides which are known to be rather flexible structures, especially in the orientation of their side chains [28].

**Table 2. Main conformational angles of the time-averaged MD conformation from the last 30-ps restrained-MD simulation.**

| Residue | $\varphi$ | $\psi$ | $\chi^1$ | $\chi^2$ | $\chi^3$ | $\gamma^4$ |
|---|---|---|---|---|---|---|
| | ° | | | | | |
| Y91 | | −79 | 65 | −80 | | |
| L92 | −158 | −33 | −173 | −63, 175 | | |
| G93 | − 48 | −26 | | | | |
| Y94 | −146 | −23 | 65 | −75 | | |
| L95 | − 62 | −21 | − 54 | −63, 175 | | |
| E96 | − 36 | −51 | 169 | 58 | 65 | |
| Q97 | − 62 | −32 | −143 | 81 | 85 | |
| L98 | − 74 | −15 | −163 | 68, −170 | | |
| L99 | − 83 | −60 | − 62 | −66, 174 | | |
| R100 | −166 | | 67 | −72 | 93 | 179 |

The torsional angles of the average conformation are given in Table 2. Except for L92, Y94, and L99, the $\phi$, $\psi$ angles are rather close to the values typical of $3_{10}$ or $\alpha$ helices. The short NH to O distances typical of hydrogen bonding (Table 3) show

**Table 3. Dimensions and occurrence of the hydrogen bonds in $\alpha_{S1}$-casein(91–100)-peptide during the last 30-ps restrained-MD simulation.**

| Donor | Acceptor | Hydrogen bond type | N-H · O bond | | Occurrence |
|---|---|---|---|---|---|
| | | | distance | angle | |
| | | | nm | ° | % |
| E96 NH | L92 CO | $i+4 \rightarrow i$ | 0.278 | 132 | 68 |
| Q97 NH | Y94 CO | $i+3 \rightarrow i$ | 0.280 | 137 | 90 |
| L98 NH | L95 CO | $i+3 \rightarrow i$ | 0.318 | 125 | 67 |
| L99 NH | E96 CO | $i+3 \rightarrow i$ | 0.285 | 134 | 74 |
| R100 NH | E96 CO | $i+4 \rightarrow i$ | 0.263 | 170 | 90 |
| R100 NεH | R100 $CO_2^-$ | | 0.282 | 144 | 98 |
| R100 Nη'H | E96 Cδ$O_2^-$ | | 0.295 | 114 | 75 |

a series of three consecutive $i+3 \rightarrow i$ interactions encompassing the Y95-L-E-Q-L-L99 sequence, preceded and followed by $i+4 \rightarrow i$ interactions typical of an $\alpha$ turn. These results confirm that the decapeptide in the SDS micellar environment assumes a helicoid conformation that is essentially of the $3_{10}$ type.

The ionic interactions R100-NεH to R100-$CO_2^-$ and R100-Nη to H-E96-Cδ$O_2^-$ are in agreement with the small temperature coefficients indicated for these guanidinium resonances. An ionic interaction between an arginine guanidinium and an aspartic or glutamic carboxylate three or four residues ahead is known to be an important helix-promoting factor [29]. This is confirmed in the present case by comparing the CD spectrum evolution upon SDS addition for the natural peptide and its [Ala100]-analog (data not shown). The transition from a random to an ordered helicoid structure is much more rapid for the former than for the latter.

The time-averaged structure exhibits an amphiphilic character, evidenced by the clustered Y91, L92, Y94, L95, L98 and L99 hydrophobic side chains on one side of the molecule, while the three hydrophilic residues (E96, Q97 and R100) are on the other side. Such an amphiphilic structure may favor its interaction with the apolar core of the micelles [30, 31],which are a rough approximation of the cellular membrane in which the benzodiazepine receptor is anchored.

**Comments.** Although the affinity of the decapeptide to the type-A 4Abu receptor is much lower than that of the benzodiazepines [32], their recognition by the same site of the receptor suggests that they share common structural properties.

Benzodiazepine agonists [14, 15] contain one seven-membered diazepam ring A, which is in a boat conformation, and two nearly planar phenyl rings B (fused to A) and C (connected by one bond to A; Fig. 6). Structure/activity relationships for benzodiazepines emphasize the importance of the relative orientation of the two aromatic rings B and C, of the presence of an electroattracting group on B, and, to a lesser extent of the carbonyl in A. Although C may rotate around the bond connecting it to A, and A may experience an inversion of boat concavity, the distance between the centers of rings B and C is constant, and equal to 0.515 nm in the crystal structure of nitrazepam [33].

In $\alpha_{S1}$-casein-(91–100)-peptide, the tyrosine aromatic rings can be related to the mandatory aromatic rings B and C in the benzodiazepine agonists, and are predicted to be at a short distance (Fig. 5). Although there are less backbone/side chain than backbone/backbone NOE connectivities, Fig. 3 lists various NOE correlations between the protons of each tyrosine side chain with the NH and Cα'H of adjacent residues. By taking these experimental constants into account in the MD simulation,

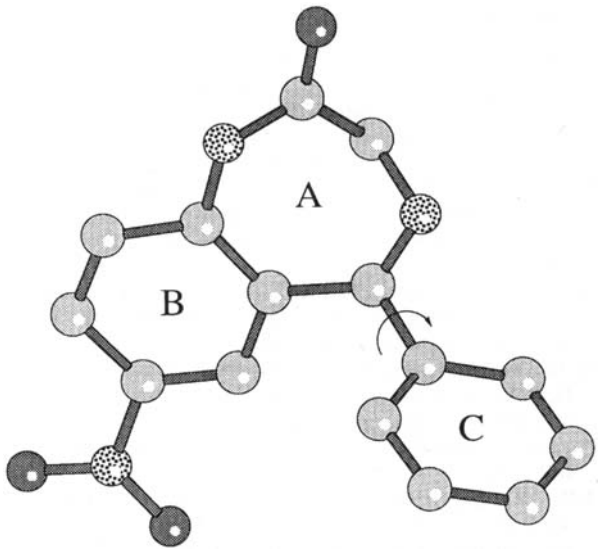


**Fig. 6. Crystal structure of nitrazepam, a benzodiazepine derivative [33].** In solution, ring C may rotate with reference to the diazepine ring A.

we observe that the distance between the tyrosine centers fluctuates in the rather narrow 0.50–0.67-nm range during the last 30-ps MD analysis, with a time-average value of 0.56 nm. The distance of 0.515 nm between the centers of B and C in nitrazepam can be found in the 0.50–0.61-nm range described above. Therefore, the flexible tyrosine rings in $\alpha_{S1}$-casein-(91–100)-peptide can easily adopt, upon recognition by the type-A 4Abu receptor, a relative disposition similar to that of the aromatic rings in the rigid benzodiazepine agonists.

## CONCLUSION

The conformation of the bovine $\alpha_{S1}$-casein-(91–100)-peptide (YLGYLEQLLR) has been determined in SDS/water micellar medium by two-dimensional-NMR and restrained-MD simulations. The time-averaged structure of the decapeptide is in good agreement with the NMR and CD data. The G93-LEQL-L99 sequence adopts a $3_{10}$-helix structure initiated and terminated by an $\alpha$ turn. The hydrophobic side chains (two tyrosine and four leucine residues) are located on the same side of the molecule, while the hydrophilic side chains (glutamine, glutamic acid and arginine residues) are situated on the other face, giving the decapeptide an amphiphilic character compatible with its interaction with SDS micelles. The ionic interactions between the R100 guanidinium and the R100 and E96 carboxylates illustrate the key role of the C-terminal Arg residue in the stabilization of the helix structure.

The substitution of an alanine for the R100 residue results in a decrease of helical propensity in the SDS/water medium, compared with that of the natural sequence. In the helicoid structure of the decapeptide, the two tyrosine aromatic cycles are oriented so that the distance between their centers and that between the centers of the benzodiazepine aromatic rings have comparable values. This might explain the affinity of $\alpha_{S1}$-casein-(91–100)peptide for the type-A 4Abu reptor.

This work was supported by the *Centre National de la Recherche Scientifique* (CNRS). A doctoral fellowship from the CNRS and the *Région Lorraine* is warmly acknowledged by CF. LM acknowledges support from the *Prospérité Fermière* (Arras, France) and the *Ministère de la Recherche et de la Technologie*.

## REFERENCES


1. Lönnerdal, B. (1985) Biochemistry and physiological function of human milk proteins, *Am. J. Clin. Nutr. 42*, 1299–1317.
2. Brantl, V. & Teschemacher, H. (1979) A material with opioid activity in bovine milk and milk products, *Naunyn-Schmiedeberg's Arch. Pharmacol. 306*, 301–304.
3. Yoshikawa, M., Tani, F., Ashikaga, T., Yoshimura, T. & Chiba, H. (1986) Purification and characterization of an opioid antagonist from peptic digest of bovine k-casein, *Agric. Biol. Chem. 50*, 2951–2954.
4. Maruyama, S. & Suzuki, H. (1982) A peptide inhibitor of angiotensine I converting enzyme in the tryptic hydrolysate of casein, *Agric. Biol. Chem. 46*, 1393–1394.
5. Parker, F., Migliore-Samour, D., Floc'h, F., Zerial, A., Werner, G. H., Jollès, J., Casaretto, M., Zahn, H. & Jollès, P. (1984) Immunostimulating hexapeptide from human casein: aminoacid sequence, synthesis and biological properties, *Eur. J. Biochem. 145*, 677–682.
6. Jollès, P., Levy-Toledano, S., Fiat, A.-M., Soria, C., Gillessen, D., Thomaidis, A., Dunn, F. W. & Caen, J. P. (1986) Analogy between fibrinogen and casein. Effect of an undecapeptide isolated from k-casein on platelet function, *Eur. J. Biochem. 158*, 379–382.
7. Lee, Y. Z., Noguchi, T. & Naito, H. (1979) An enhanced intestinal absorption of calcium in the rat directly attributed to dietary casein, *Agric. Biol. Chem. 43*, 2009–2011.
8. Azuma, N., Nagaune, S., Ishino, Y., Mori, H., Kaminogawa, S. & Yamauchi, K. (1989) DNA-synthesis stimulating peptides from human β-casein, *Agric. Biol. Chem. 53*, 2631–2634.
9. Zucht, H. D., Raida, M., Adermann, K., Magert, H. J. & Forssmann, W. G. (1995) Casocidin-I: a casein-alpha s2 derived peptide exhibits antibacterial activity, *FEBS Lett. 375*, 185–188.
10. Yamamoto, N., Akino, A. & Takano, T. (1994) Antihypertensive effect of peptides derived from casein by an extracellular proteinase from *Lactobacillus helveticus* CP790, *J. Dairy Sci. 77*, 917–922.
11. Miclo, L., Perrin, E., Driou, A., Iung, C., Boudier, J.-F. & Linden, G. (1995) Use of a benzodiazepine-like decapeptide for the preparation of drugs and food additives, European patent no. 95-02-697.7-2105.
12. Olsen, R. W. & Venter, J. C. (1986) *Benzodiazepine/GABA receptors and chloride channels: structural and functional properties*, Alan R. Liss, New York.
13. Deber, C. M. & Behnam, B. A. (1984) Role of membrane lipids in peptide hormone function: binding of enkephalins to micelles, *Proc. Natl Acad. Sci. USA 81*, 61–65.
14. Haefely, W. E., Martin, J. R., Richards, J. G. & Schoch, P. (1993) The multiplicity of actions of benzodiazepine receptor ligands, *Can. J. Psychiatry 38*, 102–108.
15. Schove, L. T., Perez, J. J. & Loew, G. H. (1994) Molecular determinants of recognition and activation at the cerebellar benzodiazepine receptor site, *Biorg. Med. Chem. 2*, 1029–1049.
16. Marion, D. & Wüthrich, K. (1983) Application of phase sensitive two-dimensional correlated spectroscopy (COSY) for measurements of $^1$H-$^1$H spin-spin coupling constants in proteins, *Biochem. Biophys. Res. Commun. 113*, 967–974.
17. Wüthrich, K. (1976) *NMR in biological research: peptides and proteins*, North-Holland, Amsterdam.
18. Piotto, M., Saudek, V. & Sklenar, V. (1992) Gradient-tailored excitation for single- quantum NMR spectroscopy of aqueous solutions, *J. Biomol. NMR 2*, 661–666.
19. Fasman, G. D. (1996) *Circular dichroism and the conformational analysis of biomolecules*, Plenum Press, New York.
20. Manning, M. C. & Woody, R. W. (1991) Theoretical CD studies of polypeptide helices: examination of important electronic and geometric factors, *Biopolymers 31*, 569–586.
21. Chakrabartty, A., Kortemme, T., Padmanabhan, S. & Baldwin, R. L. (1993) Aromatic side-chain contribution to far-ultraviolet circular dichroism of helical peptides and its effect on measurement of helix propensities, *Biochemistry 32*, 5560–5565.
22. Billeter, M., Braun, W. & Wüthrich, K. (1982) Sequential resonance assignments in protein nuclear magnetic resonance spectra. Computation of sterically allowed proton-proton distances and statistical analysis of proton-proton distances in single crystal protein conformations, *J. Mol. Biol. 155*, 321–346.
23. Tsikaris, V., Tzovaras, D., Sakarellos-Daitsiotis, M., Sakarellos, C., Orlewski, P., Cung, M. T. & Marraud, M. (1996) Isomerization of the Xaa-Pro peptide bond induced by ionic interaction of arginine, *Biopolymers 38*, 673–682.
24. Wüthrich, K. (1986) *NOE-observable $^1$H-$^1$H distances in proteins*, John Wiley & Sons, New York.
25. Sutcliffe, M. J. (1993) Structure determination from NMR data II. Computational approaches, in *NMR of macromolecules* (Roberts, G. C. K., ed.) pp. 359–390, Oxford University Press, New York.
26. Sejbal, J., Cann, J. R., Stewart, J. M., Gera, L. & Kotovych, G. (1996) An NMR, CD, molecular dynamics, and fluorometric study of the conformation of the bradykinin antagonist B-9340 in water and in aqueous micellar solutions, *J. Med. Chem. 39*, 1281–1292.
27. Zetta, L., Consonni, R., Demarco, A., Longhi, R., Manera, E. & Vecchio, G. (1990) Opioid peptides in micellar systems: conformational analysis by CD and by one-dimensional and two-dimensional $^1$H-NMR spectroscopy, 899–909.
28. Geyer, A., Müller, G. & Kessler, H. (1994) Conformational analysis of a cyclic RGD peptide containing a $\psi$[$CH_2$-NH] bond: a positional shift in backbone structure caused by a single dipeptide mimetic, *J. Am. Chem. Soc. 116*, 7735–7743.
29. Scholtz, J. R. M. & Baldwin, R. L. (1992) The mechanism of α-helix formation by peptides, *Annu. Rev. Biophys. Biomol. Struct. 21*, 95–118.
30. Jung, H., Windhaber, R., Palm, D. & Schnackerz, K. D. (1996) Conformation of a beta-adrenoceptor-derived signal transducing peptide as inferred by circular dichroism and $^1$H NMR spectroscopy, *Biochemistry 35*, 6399–6405.
31. Bairaktari, E., Mierke, D. F., Mammi, S. & Peggion, E. (1990) Conformational studies by circular dichroism, $^1$H NMR, and computer simulations of bombolitins I and III in aqueous solution containing surfactant micelles, *Biochemistry 29*, 10090–10096.
32. Müller, W. E. (1987) *Benzodiazepine receptor: drug acceptor only of a physiologically relevant part of our central nervous system?* Cambridge University Press, Cambridge.
33. Gilli, G., Bertolasi, V., Sacerdoti, M. & Borea, P. A. (1977) 7-Nitro-1,3-dihydro-5-phenyl-2H-1,4-benzodiazepin-2-one (Nitrazepam), *Acta Cryst. Ser. B 33*, 2664–2667.


*Note added in proof.* The bioactive peptides from milk have been reviewed recently [Teschemacher, H., Koch, G. & Brantl, V. (1997) Milk protein-derived opioid receptor ligands, *Biopolym. Pept. Sci. 43*, 99–117; Meisel, H. (1997) Biochemical properties of regulatory peptides derived from milk proteins, *Biopolym. Pept. Sci. 43*, 119–128]. The bifurcated hydrogen bonds in two intermediate $3_{10}/\alpha$ helices have been described recently [Datta, S., Shamala, N., Banerjee, A. & Balaram, P. (1997) Hydrogen bonds in peptide helices. Analysis of two independent helices in the crystal structures of a peptide Boc-Val-Ala-Leu-Aib-Val-Ala-Phe-OMe, *J. Pept. Res. 49*, 604–611].